ELSEVIER

Colloids and Surfaces
A: Physicochemical and Engineering Aspects 132 (1998) 31–44

COLLOIDS AND SURFACES A

Synthesis and characterization of catalytic titanias via hydrolysis of titanium(IV) isopropoxide

Kamal M.S. Khalil [a,1], Thomas Baird [a], Mohamed I. Zaki [b,*], Ahmed A. El-Samahy [c], Aida M. Awad [c]

[a] *Electron Microscopy Centre, Department of Chemistry, Glasgow University, Glasgow, G12 8QQ, UK*
[b] *Chemistry Department, Faculty of Science, Kuwait University, PO Box 5969, Safat 13060, Kuwait*
[c] *Department of Chemistry, Faculty of Science, South Valley University, Sohag 82524, Egypt*

Received 1 October 1996; accepted 24 April 1997

Abstract

Transmission electron microscopy (TEM) studies and nitrogen gas adsorption data were used to investigate textural characteristics of titanias prepared via calcination, at 400°C/3 h, of the hydrolysis products of titanium(IV) isopropoxide in *n*-heptane or isopropanol solvent. A variety of titanias (anatase form) were produced with different textural characteristics. The nature of these products was controlled largely by the synthesis parameters such as water ratio, the addition of acetic acid, and the solvent used during the hydrolysis. The resultant microstructure of the solids is correlated with the pertinent preparative conditions. © 1998 Elsevier Science B.V.

Keywords: Titania; Catalytic titania; Hydrolysis of Titanium(IV) isopropoxide

1. Introduction

Titania, TiO_2, has diverse applications in the field of heterogeneous catalysis. It is used as a catalyst [1,2], a support of a number of monolayer-type metal [3] and metal oxide [4] catalysts, and a promoter for environmental catalysts [5]. Consequently, it is important to obtain titania of high surface area, and uniform particle size and pore structure. Conventionally, titania is prepared from inorganic precursors, mainly by thermal hydrolysis of titanium(IV) compounds in highly acidic solutions, or by thermal oxidation of $TiCl_4$ vapour at high temperature regimes [6]. Recently, however, methods of vapour-phase hydrolysis [7] and pyrolysis [8], and sol-gel processing [9,10] of organic precursors, namely titanium(IV) isopropoxide, have been developed to synthesize titanias of favourable textural properties.

In the sol-gel method [11] a variety of titanium(IV) alkoxides ($Ti(OR)_4$) are dispersed in non-reactive organic solvents and then hydrolysed. The properties and nature of the product are controlled by the particular alkoxide used, the presence of acidic or basic additives, the solvent, and various other processing conditions (e.g. temperature, stirring, etc.). The chemistry involved is rather complex. Reactions such as hydrolysis, esterification, alcoholic condensation, water condensation, and alcoholysis occur successively and consecutively, and lead eventually to dispersed gel or a precipitate [12].

* Corresponding author.

[1] On leave from: Department of Chemistry, Faculty of Science, South Valley University, Sohag 82524, Egypt.

PII S0927-7757(97)00156-8

Previous research has been devoted mainly to understanding equilibria involved in the sol→gel processing of metal alkoxides in general [11–14], and titanium alkoxide in particular [14].

The present studies were carried out to gain a detailed knowledge of the microstructures of titanias formed under different conditions via the sol-gel process and to try to equate observed structural features with the prevailing processing conditions. A comparison is made of titanias prepared by hydrolysis of titanium(IV) isopropoxide, $Ti(OPr^i)_4$, in *n*-heptane and isopropanol solvents using various alkoxy/water ratios. Subsequent calcination (400°C/3 h) of the hydrolysis products yielded the titanias. In some experiments acetic acid additions were made to promote precursors whose modified molecular structures would undoubtedly influence the ultimate microstructures of the titania products. Sanchez et al. [14], for example, showed that acetic acid additions gave hydrolysis products of $Ti(OPr^i)_4$ that contained both alkoxy and acetate groups, the latter being the more difficult to remove on further hydrolysis. The use of *n*-heptane and isopropanol solvents was made to provide heterogeneous and homogeneous synthesis routes respectively, for comparison, water being immiscible with *n*-heptane. Different titania microstructures might thus be expected from these two systems. High resolution electron microscopy was used to provide direct visual evidence of the microstructure of TiO_2 products formed in this series of experiments, and nitrogen adsorption isotherms were used to ascertain the surface texture (surface area and porosity). The results of the two techniques are compared and the overall findings are correlated with the appropriate preparative conditions and with mechanistic viewpoints derived from previous literature.

2. Experimental

2.1. Materials

The titanium(IV) isopropoxide ($Ti(OPr^i)_4$) used was 99.9% pure liquid (Aldrich (USA)). Solvents of 99.99% pure *n*-heptane (C_7H_{16}) and isopropanol (C_3H_7OH) and 99.5% pure acetic acid (CH_3COOH) were all Aldrich products, and used as supplied. Nitrogen gas was 99.9% pure as supplied (Aswan Gases Company, Egypt). It was further purified by passing it through a packed column of reduced copper heated to 350°C.

The hydrolysis of the alkoxide was carried out by the dropwise addition of a calculated amount of bi-distilled water to a 200-ml portion of 0.4 M solution of the alkoxide in *n*-heptane (or isopropanol) being magnetically stirred at 400 rev min^{-1} at ambient temperature. The amount of water was varied to maintain water/alkoxy molar ratios of 1, 2 and 8. In a separate preparation scheme a calculated amount of acetic acid solution (4 M) was added to the alkoxide solution prior to addition of water. Acetic acid/alkoxy molar ratios of 0.125, 0.25, and 1 were employed. The solution was kept magnetically stirred for 1 h (for just 1 min in the case of isopropanol solvent), followed by ageing at ambient temperature. After 3 days the hydrolysis product, which occupied about half of the original solution volume, was filtered off using Whatman filter paper, and the resulting gel was allowed to dry overnight at ambient temperature. The dried gel was ground and then allowed to dry further at 60°C for 24 h to give the titania precursor materials used in this work. For clarity, dried hydrolysis products in *n*-heptane are denoted by "SH", whereas those obtained in isopropanol are designated "SP". Arabic numerals are added to these designations to indicate the molar composition at hydrolysis. Hence SH(1:1:0.125) indicates the hydrolysis product of the alkoxide dissolved in *n*-heptane at alkoxide/water/acid molar ratio of (1:1:0.125). Table 1 summarizes the hydrolysis products and their preparation ratios, designations and carbon analysis results. Calcination of the hydrolysis products was done by heating for 3 h at 400°C in a static atmosphere of air. The calcination products are designated similarly to the parent hydrolysis products, although omitting the letter "S". Thus H(1:1:0.125) is the 400°C calcination product of SH(1:1:0.125).

2.2. Thermal analysis

The titania precursors were subjected to thermogravimetry (TG) using a Du Pont 990 analyser

Table 1
The alkoxide hydrolysis products (i.e. titania precursors), and their preparation ratios, designations, and carbon analysis results

Hydrolysis product	Molar ratio[a] alkoxy:water:acetic acid		Carbon mass (%)
SH(1:1:0)	1:1:0	in *n*-heptane	0
SH(1:2:0)	1:2:0	in *n*-heptane	0
SH(1:8:0)	1:8:0	in *n*-heptane	0
SH(1:1:0.125)	1:1:0.125	in *n*-heptane	8.3
SH(1:1:0.25)	1:1:0.25	in *n*-heptane	10.5
SH(1:1:1)	1:1:1	in *n*-heptane	18.0
SP(1:1:0)	1:1:0	in isopropanol	1.0
SP(1:2:0)	1:2:0	in isopropanol	1.0
SP(1:8:0)	1:8:0	in isopropanol	1.9
SP(1:1:0.125)	1:1:0.125	in isopropanol	7.8
SP(1:1:0.25)	1:1:0.25	in isopropanol	9.4
SP(1:1:1)	1:1:1	in isopropanol	16.3

[a] For instance, 2.2 mL of water + 300 mL of 0.4 M isopropoxide gives alkoxy:water of 1:1 molar ratio.

combined with a 951 thermobalance. 20–25 mg portions of test materials were placed in a small platinum boat in a stream of nitrogen gas (20 ml min^{-1}), and heated at 10°C min^{-1} up to 600°C.

2.3. Bulk analysis

Bulk properties of the hydrolysis and calcination products were established by infrared spectroscopy, and X-ray and electron diffractometry. IR spectra were taken from KBr-supported disks of test materials over the range 4000–400 cm^{-1} with a resolution of 4 cm^{-1} using a model 983 Perkin–Elmer spectrophotometer. X-ray powder diffractograms were measured using a Philips diffractometer, and a CuKα radiation source. X-ray diffraction (XRD) patterns derived therefrom were matched with ASTM standards [15] for identification of phase and chemical compositions. Carbon analyses were performed in duplicate with a 110b Carlo Erba analyser using 1 mg samples.

2.4. Texture assessment

The surface area ($S/m^2\ g^{-1}$) was determined by BET analysis [16] of nitrogen adsorption isotherms, measured on test materials at liquid nitrogen temperature, using a conventional volumetric method [17]. Test materials were thoroughly outgassed for 2 h and cooled to liquid nitrogen temperature prior to exposure to the nitrogen adsorptive. The pore structure was assessed by application of the *n*-method of Lecloux and Pirard [18] in which deviations from linearity of V_a–n plots are indicative of the types of pore present (V_a is the adsorbed volume; $n = V_a/V_m$, where V_m is calculated from the BET equation). Pore sizes were calculated [19] from the nitrogen adsorption data.

Transmission electron microscopy (TEM) was also used to characterize the solids. Test samples were prepared by ultrasonic dispersion of the powder in isopropanol and then a drop of the suspension was placed on to carbon-coated grids or perforated carbon films. The latter were used to eliminate phase contrast effects arising from the carbon support film and permitted clear lattice images to be obtained from the samples by photographing regions that extended over the holes. Care was taken to minimize the risk of radiation damage to the solids whilst viewing, and indeed this was found to be negligible under the investigation conditions used in this work. A model 002B Akashi (Japan) microscope, operated at 200 kV, was utilized in this work. An LaB_6 filament was used as a coherent illumination source for high resolution work. Selected-area electron diffraction (ED) patterns were taken whenever required to gain structural information about test materials. Lattice spacings (*d*-values) were calculated using graphite as a standard.

3. Results

3.1. The carbon content

Table 1 shows that the hydrolysis products of $Ti(OPr^i)_4$ in *n*-heptane contain no carbon at detectable levels (measurements were accurate to within ±0.2%). In isopropanol at corresponding water ratios the hydrolysis products contain 1–2% carbon. In both solvents, however, the addition of acetic acid resulted in hydrolysis products that

retained increasing amounts of carbon (7.8–18.0%) with increase in acid concentration. Further analysis (see Section 3.3) revealed the presence of organic groups as the source of the carbon. Thus, the presence of the acid additives evidently hampers significantly the hydrolysis sequence of the alkoxide. When heated in air at 400°C for 3 h the hydrolysis products gave materials that were carbon free.

3.2. Thermal analysis

Fig. 1 displays representative TG curves which were obtained for hydrolysis products of the alkoxide in the absence (SH(1:1:0)) and in the presence (SH(1:1:0.25)) of acetic acid. They are typical results irrespective of the solvent used and the water ratio. In the absence of acid the TG curve monitors the slow and gradual weight loss of ca. 20–21% that occurs on heating up to 300°C. In the presence of acid the total weight loss is increased to 33–44% with the emergence of a second weight loss step of high rate maximized near 300°C. The loss involved in the second step amounts to 13–24%, the higher values being obtained with higher acid concentrations.

The above results for the decomposition of the hydrolysis products in the absence of the acid indicate the formation of a thermally stable material at >220°C. As carbon species were not detected in the test materials (Table 1) the volatile component is most probably water of hydration. A stoichiometric calculation based on the weight loss determined, 20–21%, accounts for the elimination of about 1.2 mol of water. The second weight loss step appearing in the presence of the acid may be related to the organic species responsible for the carbon masses detected in these materials (Table 1). Thus these carbon-containing species are chemically uniform, either isopropoxide or acetate, being driven off in a well-defined temperature region $T_{max} \approx 300$°C.

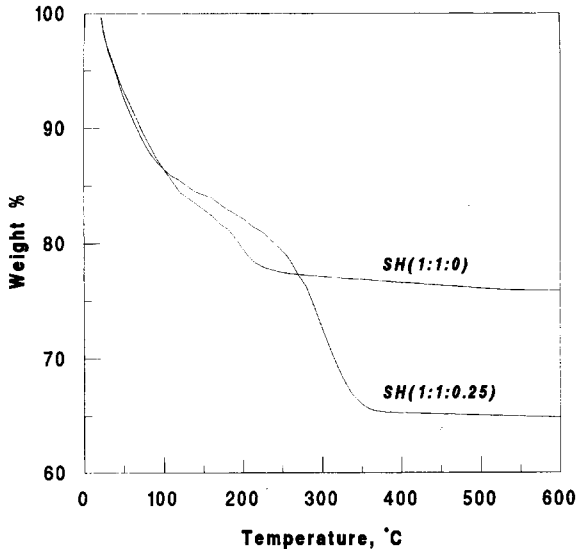

Fig. 1. TG curves obtained by heating the indicated hydrolysis products at 10°C min^{-1} in 30 ml min^{-1} flow of N_2.

3.3. IR spectra

Typical IR spectra exhibited by the hydrolysis products (and their calcination products at 400°C) in the absence and in the presence of acetic acid are shown for the indicated materials in Fig. 2. In the absence of the acid the spectra of the hydrolysis products were completely free of absorptions due to isopropoxide groups. They show only absorption due to νOH at 3420 cm^{-1}, δHOH at 1624 cm^{-1} and νTi–O (at <1200 cm^{-1}) vibrations. These results confirm that the hydrolysis products in the absence of the acid contain freely bending water molecules.

In the presence of the acid, moreover, the spectra

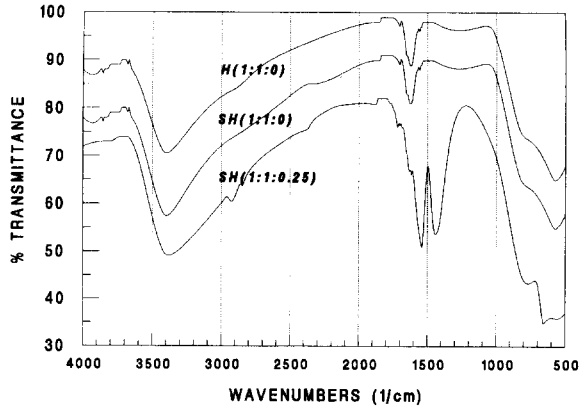

Fig. 2. Typical IR spectra of some hydrolysis products and calcined material.

show a strong band structure consisting of two strong absorptions occurring around 1500 cm^{-1}; these are diagnostic of $\nu_{sy}COO^-$ and $\nu_{asy}COO^-$ modes of vibration of the acetate groups [20]. Additional absorption bands at lower frequencies are also relevant to the presence of acetates. The spectra thus confirm that the original isopropoxide groups are replaced by water molecules and acetate groups. Accordingly, the second weight loss step exhibited by the test materials (e.g. SH(1:1:0.25), in Fig. 1) is due to elimination of the acetate groups. Hence the absence of acetate absorptions in the spectra taken from the calcination products (at 400°C) of the hydrolysis products is understandable. The spectra also indicate (Fig. 2) that dehydration is effected throughout the calcination course, and that the end-product is mostly titanium oxide exposing hydroxylated surfaces (cf. the νOH absorption at 3420 cm^{-1}).

3.4. X-ray powder diffractograms

The hydrolysis products, in general, were non-crystalline to XRD. The diffractogram shown for H(1:1:0.25) in Fig. 3 is typical of all of the calcination products, irrespective of the preparation course. It displays a diffraction pattern characteristic of anatase titania [15]. The diffraction peaks displayed are rather broad, thus indicating small crystallites.

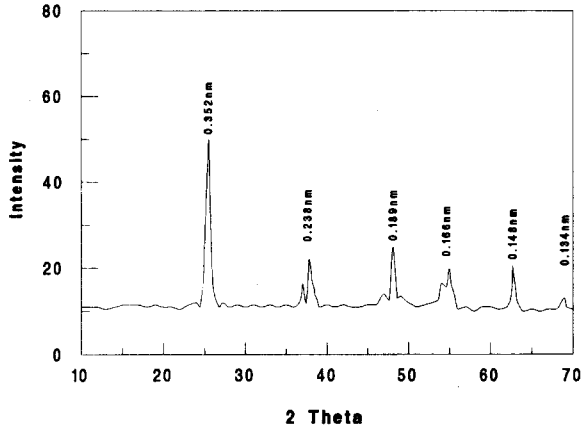

Fig. 3. X-ray diffractogram typical of calcined material; *d*-values correspond with those of anatase.

3.5. Nitrogen adsorption isotherms

Nitrogen adsorption was determined on the various titanias (i.e. calcined hydrolysis products) obtained under varied preparation conditions. The resulting isotherms are shown for the preparations done in *n*-heptane and isopropanol in Figs. 4 and 5 respectively, both in the absence and presence of acid additives. The isotherms are generally of type IV and exhibit hysteresis mostly of type H2. Thus the materials are mesoporous and the pores are networked [17,19]. It is worth noting that titanias derived from materials prepared at the highest acid ratio in both solvents exhibit uniquely type H3 hysteresis, which arises from ink-bottle-shaped pores [17,19].

The BET analysis results are cited in Table 2. It is obvious that the hydrolysis products of the alkoxide solution in *n*-heptane lead to high surface area titanias ($\geq 115\ m^2\ g^{-1}$). The acid additive reduces significantly the surface area ($\leq 65\ m^2\ g^{-1}$). On the other hand the hydrolysis

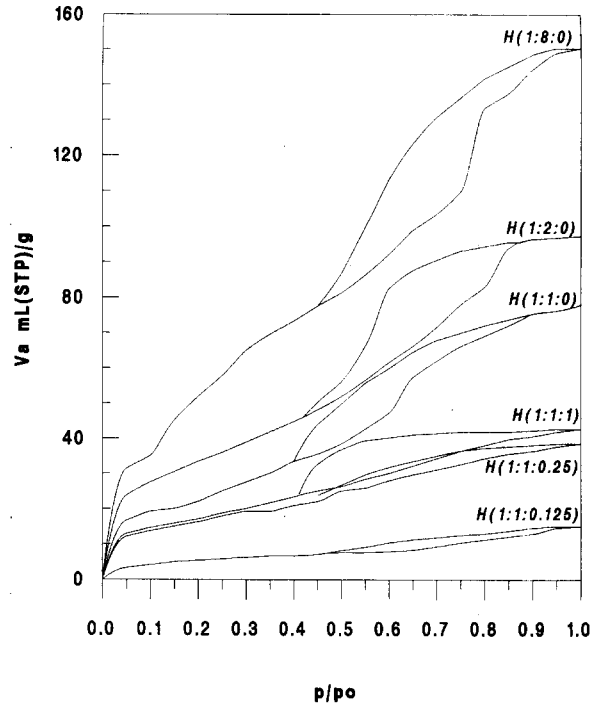

Fig. 4. N_2 adsorption isotherms obtained from calcined products ex. *n*-heptane solvent system.

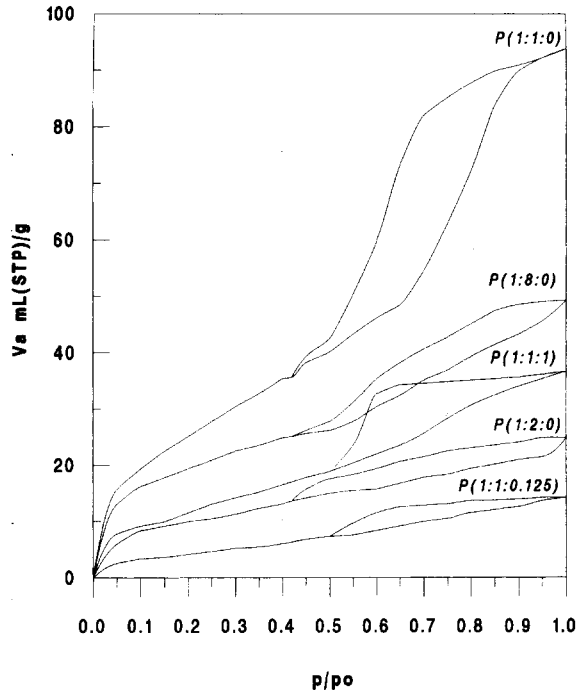

Fig. 5. N_2 adsorption isotherms obtained from calcined products ex. isopropanol solvent system.

Table 2
The specific surface area S_{BET}, the C_{BET} constant, pore type, and pore size r_p for the various titanias

Material	S_{BET}, ($m^2\,g^{-1}$)	C_{BET}	Pore type	r_p (nm)
H(1:1:0)	115	79	meso	2, 3
H(1:2:0)	126	66	meso	2, 3, 6
H(1:8:0)	151	99	meso	2, 3, 5
H(1:1:0.125)	60	178	meso	3
H(1:1:0.25)	20	78	meso + micro	2
H(1:1:1)	65	67	meso	2, 5
P(1:1:0)	102	33	meso	2, 2.5, 4
P(1:8:0)	70	93	meso + micro	2.5
P(1:1:0.125)	13	169	meso	2
P(1:1:1)	49	30	meso	2, 4

products in isopropanol result in low area titanias ($\leq 102\ m^2\,g^{-1}$). The acid additives further reduced the surface areas ($\leq 49\ m^2\,g^{-1}$). Correlating the surface area with the preparation variables shows a surface area increase with increase in water ratio in heptane, but a decrease in isopropanol.

Table 2 also shows the pore types in the titanias as derived from the *n*-analysis method [18] and calculated pore sizes based on the adsorption branch of the isotherms [19]. The results indicate that all of the titanias synthesized are mesoporous in nature, except for H(1:1:0.25) and P(1:8:0) where additional micropores, <2 nm, are implied.

3.6. TEM

TEM studies were carried out on all the solids produced by calcination of the hydrolysis precursors obtained via *n*-heptane and isopropanol solvents, both in the presence and in the absence of acetic acid as listed in Table 2. ED data obtained from all these solids were consistent with the lattice spacings of the anatase form of TiO_2. Typical *d*-values are given in Table 3.

High resolution lattice imaging of the calcined products showed in all cases lattice fringes corresponding to those of anatase, in agreement with the ED data. Lattice fringes can be seen in Figs. 7(B), 8(B), 9(A) and 9(B).

A typical electron micrograph representative of the 400°C calcination products obtained via *n*-heptane in the absence of acetic acid H(1:2:0) is shown in Fig. 6(A). The micrograph exhibits irregularly shaped titania aggregates composed of very small elementary particles of a size ranging from ~5–10 nm diameter. Fig. 6(B), a higher magnification micrograph of the same material, depicts the small discrete elementary particles more clearly and shows that they are packed together in a rather open structure. The porosity in these

Table 3
Typical electron diffraction data from calcined hydrolysis products

d-values (nm)		(*hkl*)
Experimental	ASTM [15]	
0.352	0.352	(101)
0.237	0.238	(004)
0.189	0.189	(200)
0.166	0.166	(211)
0.148	0.148	(204)
0.133	0.134	(220)

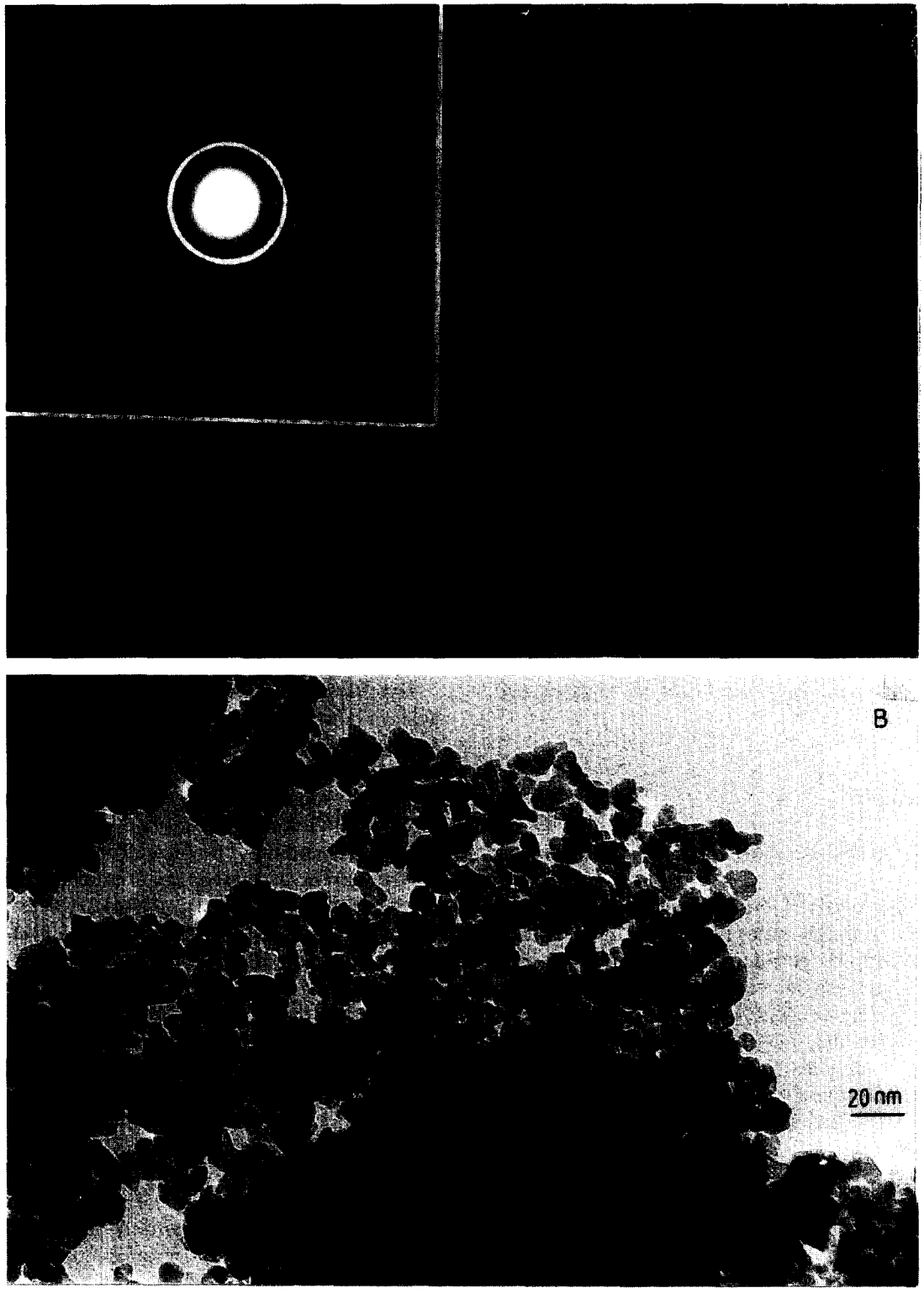

Fig. 6. (A) TEM micrograph typical of the calcination product of type H material processed in the absence of acid; (B) a higher magnification micrograph of one of the aggregates shown in (A) showing its discrete component particles.

materials appears to be in the form of interparticle voids rather than inherent crystallite porosity. Pore sizes of <2 nm and up to >50 nm can be observed at the inter-particle regions in Fig. 6(B). However, a visual estimation of pore sizes or shapes is difficult to realize due to the irregular shape of pore entrances and to the fact that the micrographs represent only a two-dimensional projection of the pores. The insert in Fig. 6(A) is a typical ED pattern of the anatase structure.

The 400°C calcination products (anatase) obtained via *n*-heptane solvent in the presence of acetic acid exhibited different morphologies from those obtained in the absence of acid. At low (H(1:1:0.125)) and medium (H(1:1:0.25)) acid ratios agglomerates of large spheroidal particles of ~ 300 nm diameter were produced, as shown for example in Fig. 7(A). At the highest acid ratio used, H(1:1:1), massive irregularly shaped aggregates were obtained, reflecting the enhanced gelation observed for the precursor products. Fig. 7(B) shows the edge profile of such material. All the TiO_2 products formed in this series of experiments (in *n*-heptane + acetic acid) consisted of large aggregates composed of compacted smaller crystallites which may be partially fused together (see Fig. 7(B)).

4. Discussion

4.1. The hydrolysis course and calcination products

The hydrolysis of $Ti(OPr^i)_4$ in *n*-heptane under the various alkoxy/water ratios used in the present studies led to the formation of carbon-free precursors. TG analysis showed the precursors lost about 20% of their original weight on calcination at 400°C. Thus they may be considered as hydrated titanium dioxide of the general formula $TiO_2.yH_2O$, where $y=1.2$. The hydrolysis reaction may be expressed as

$$Ti(OPr^i)_4 + xH_2O \rightarrow TiO_2 \cdot yH_2O + 4Pr^iOH$$

It is interesting that carbon species were not detected by carbon analysis or IR spectroscopy in the hydrolysis products formed using low water contents (e.g. SH(1:1:0); $x=1$ in the above equation) where the hydrolysis should be incomplete. A possible explanation is that the stirring rate was too low to allow immediate thorough mixing of the reactants, resulting in high local concentrations of water at the *n*-heptane/water interface. This could give rise to fully hydrolysed product at the interface (a precipitate was observed immediately on addition of water) leaving some of the $Ti(OPr^i)_4$ unhydrolysed due to slow diffusion to the interface.

Calcination (400°C/3 h) of the precursors SH(1:1:0), SH(1:2:0) and SH(1:8:0) gave (carbon-free) titanias H(1:1:0), H(1:2:0) and H(1:8:0) respectively. XRD showed that these titanias consisted solely of the anatase phase.

The hydrolysis of $Ti(OPr^i)_4$ in isopropanol led to the formation of hydrated titanium oxide SP(1:1:0), SP(1:2:0) and SP(1:8:0) just as for the materials obtained in *n*-heptane. However, all the hydrolysis products here contained small amounts of organic residues (1–2% carbon), probably as a result of the inclusion of some solvent or esterification of the hydrolysed products. Calcination of these precursors gave pure titania P(1:1:0), P(1:2:0) and P(1:8:0) of anatase structure.

Hydrolysis of $Ti(OPr^i)_4$ in the presence of acetic acid (in both solvents) gave rise to modified precursors (as shown by carbon analysis and IR spectroscopy) containing much higher concentrations of organic groups. It has been reported [21] that mono- and di-acetate-substituted alkoxides can be formed. Accordingly, low acid/Ti ratios result in the formation of isopropoxy/acetate compounds of the formula $Ti(OPr^i)_{4-x}(OAc)_x$, where $x \leq 2$. The addition of water, as in the present studies, would be expected to hydrolyse such compounds. Sanchez et al. [14], using IR and NMR techniques, showed that the alkoxy groups are first removed upon hydrolysis, while coordinated acetates remain bonded much longer. The present IR results (Fig. 2) and carbon analyses (Table 1) imply compatibly that the hydrolysis affects mainly the alkoxy groups to give presumably hydrolysis products of the formula $Ti(OR)_{(4-x-y)}(OAc)_x(OH)_y$, where $x+y \leq 4$. Calcination of these compounds leads to decomposition of both the residual alkoxy groups and the acetate groups to give pure titanium dioxide.

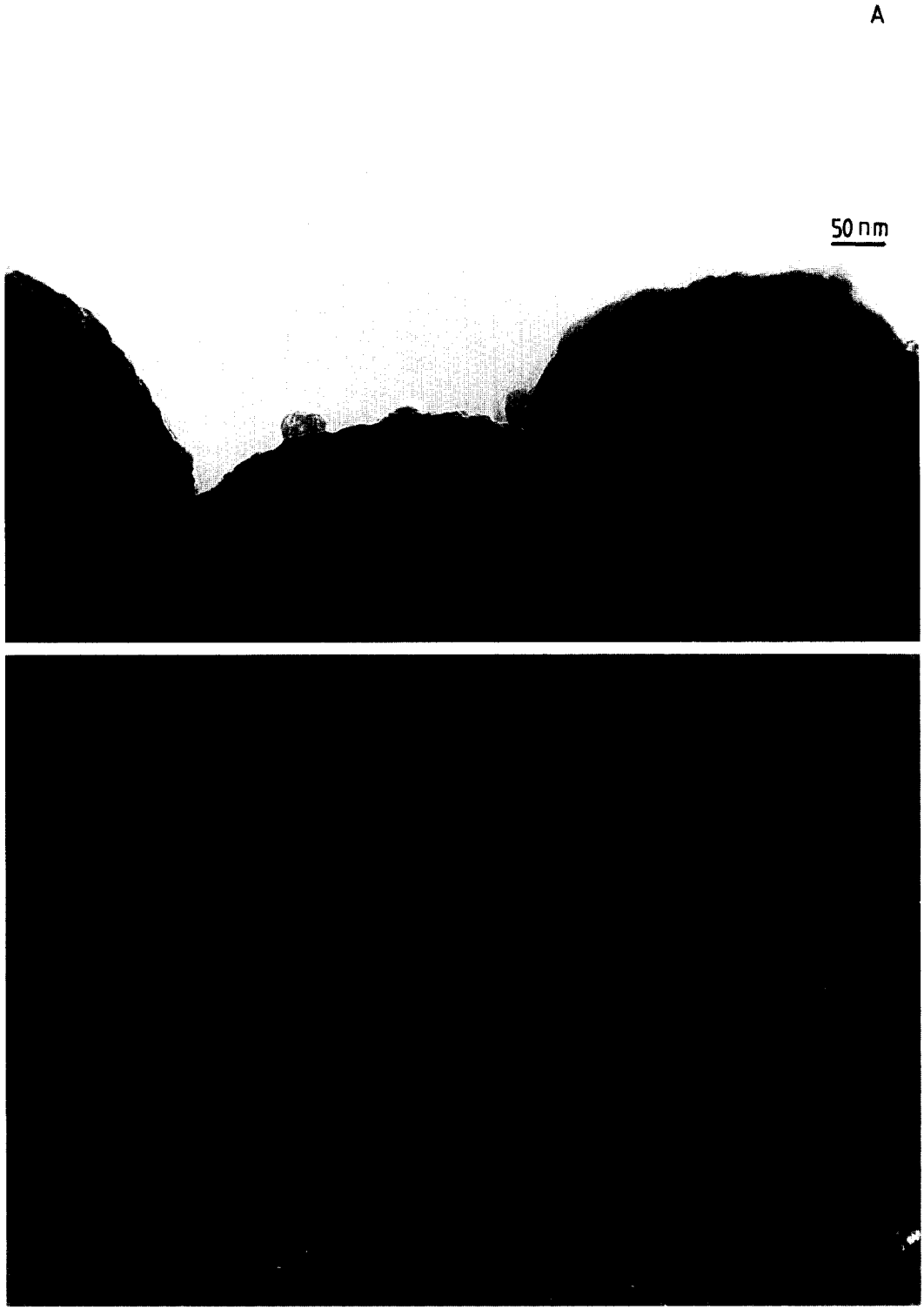

Fig. 7. (A) TEM micrograph of the large spheroidal particles typical of the H(1:1:0.25) material; (B) high resolution electron micrograph of the H(1:1:1) material showing a compact structure.

4.2. Texture evolution through processing

4.2.1. Background mechanisms

The texture of the xerogel obtained via sol-gel processing evolves sequentially as the successive product of the following hydrolysis and condensation reactions and the reverse reactions [14]:

$$\equiv Ti(OPr^i) + H_2O \underset{\leftarrow \text{esterification}}{\overset{\text{hydrolysis}\rightarrow}{=}} \equiv Ti(OH) + Pr^iOH$$

$$\equiv Ti(OH) + \equiv Ti(OH) \underset{\leftarrow \text{depolymerization}}{\overset{\text{condensation}\rightarrow}{=}} \equiv Ti-O-Ti\equiv + H_2O$$

The texture of the calcination products is determined by the nature of the hydrolysed materials which may exist as a molecular network or a colloidal sol. It was concluded [22] that four general models may be involved upon drying: (a) low cross-linked polymeric clusters give rise to a networked structure; (b) highly cross-linked clusters give rise to small aggregated particles; (c) colloidal gel aged under conditions of high solubility results in coarsening of the porosity; (d) colloidal gel composed of weakly bonded particles, under conditions of low solubility, are aggregated without coarsening of the porosity.

4.2.2. Microstructures of titanias as a function of processing conditions

4.2.2.1. Role of solvent and water content during hydrolysis. The present TEM studies showed that all of the calcination products of materials prepared in the absence of acetic acid (i.e. solvent + water only present) were composed of aggregates of small elementary particles of about the same average size. Thus, the observed differences in the present experiments, in terms of surface area and porosity of these materials (Table 2), are likely to be due to the way in which the aggregates of elementary particles are packed, since no extensive inherent meso-porosity was observed in these solids under high resolution examination by TEM, i.e. interparticle voids are of paramount importance in respect of porosity and surface area factors.

The effect of the solvent could be argued to arise from the different abilities to allow condensation and aggregation on one hand, and to stabilize the formed aggregates against precipitation on the other hand. Coalescence of particles will be controlled by both the above processes. *n*-Heptane as an aprotic solvent will have less ability to stabilize gels than isopropanol (protic solvent). Thus the aggregation rate may be expected to be faster in *n*-heptane than in isopropanol, leading to a looser packing (i.e. porous nature) in the former solvent. TEM micrographs indeed verified the above clearly, a considerably more open structure being observed for the "H"-type materials (cf. Figs. 6 and 8). This open structure may explain why all "H"-type titanias have higher surface areas than those of the corresponding "P" type.

If the above argument is acceptable, we may explain the increase of S_{BET} and porosity on going from H(1:1:0) to H(1:2:0), and further to H(1:8:0), in terms of the more heterogeneous nature of the reaction leading to a decrease in the mean size of the elementary particles with increase in water ratio, as was shown by Chen et al. [23] for silica prepared via the sol-gel process. Moreover, increasing the amount of water during the aging of the hydrolysed product may create more porosity due to the channels created on drying.

The decrease of S_{BET} and porosity for P(1:1:0) and P(1:8:0) compared with H(1:1:0) and H(1:8:0) on the one hand, and the decrease of S_{BET} for P(1:8:0) compared with P(1:1:0) on the other hand, may be interpreted in terms of an increase in the depolymerization rate in isopropanol (resulting in more dense packing). Meanwhile, the rate of coalescence may increase resulting in an increase in particle size. The observed increase in the size of the elementary particles of P(1:8:0) ($\sim$10–16 nm) in comparison to $\sim$5–10 nm for H(1:1:0) is in accord with the above interpretation.

4.2.2.2. Role of acetic acid. Titanias prepared in the presence of acetic acid, irrespective of the solvent, consisted of an extensive network of fused crystallites, as shown in the micrographs in Figs. 7 and 9, and in this respect the microstructures differed from the compacted discrete crystallites that were found in the absence of acid. Addition

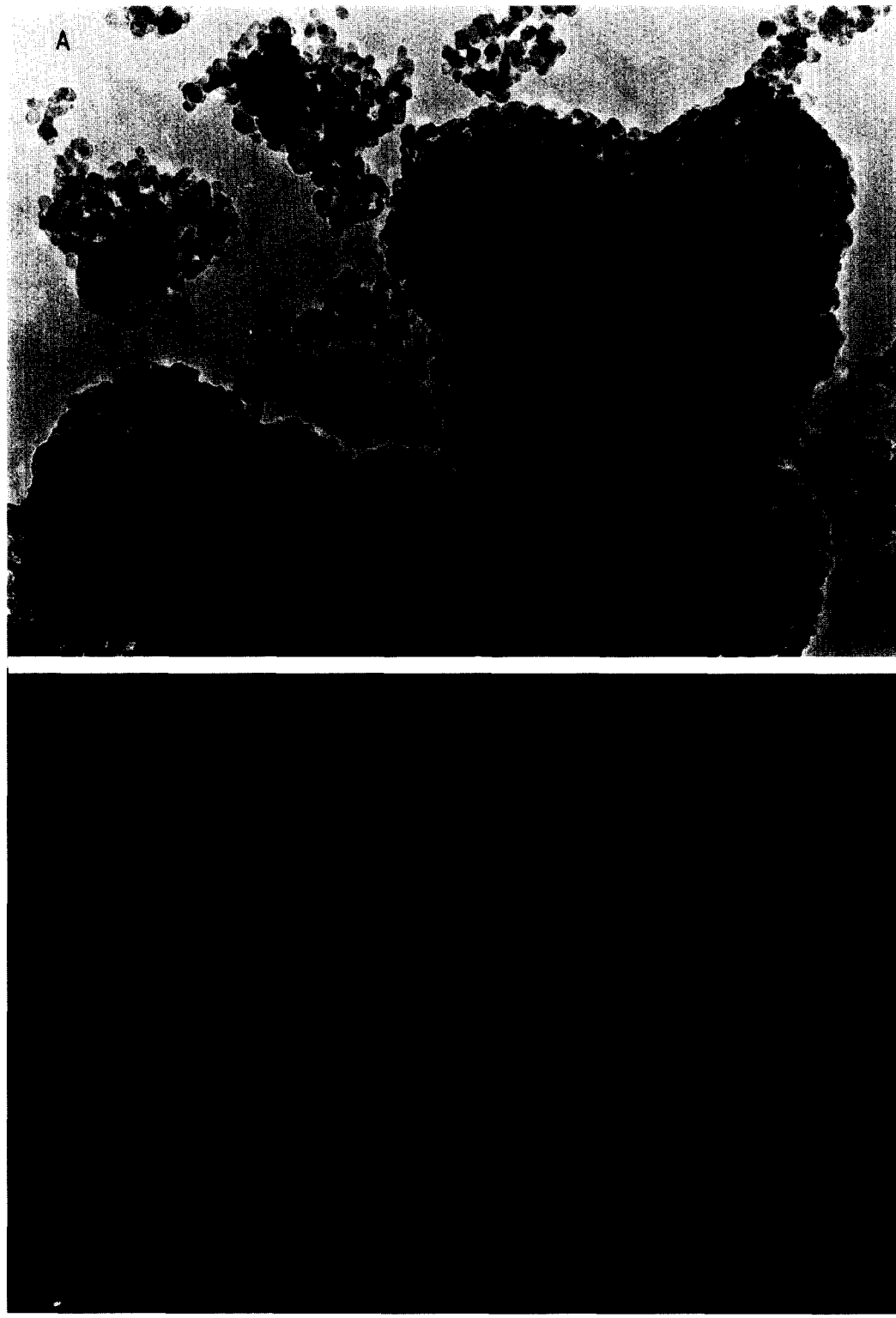

Fig. 8. (A) TEM micrograph of the calcination product of type P material processed in the absence of acid revealing aggregates of small elementary particles similar to those in Fig. 6(A); (B) a high resolution micrograph of one of the aggregates shown in (A)—lattice images corresponding to an anatase structure can be seen across the extent of individual crystallites.

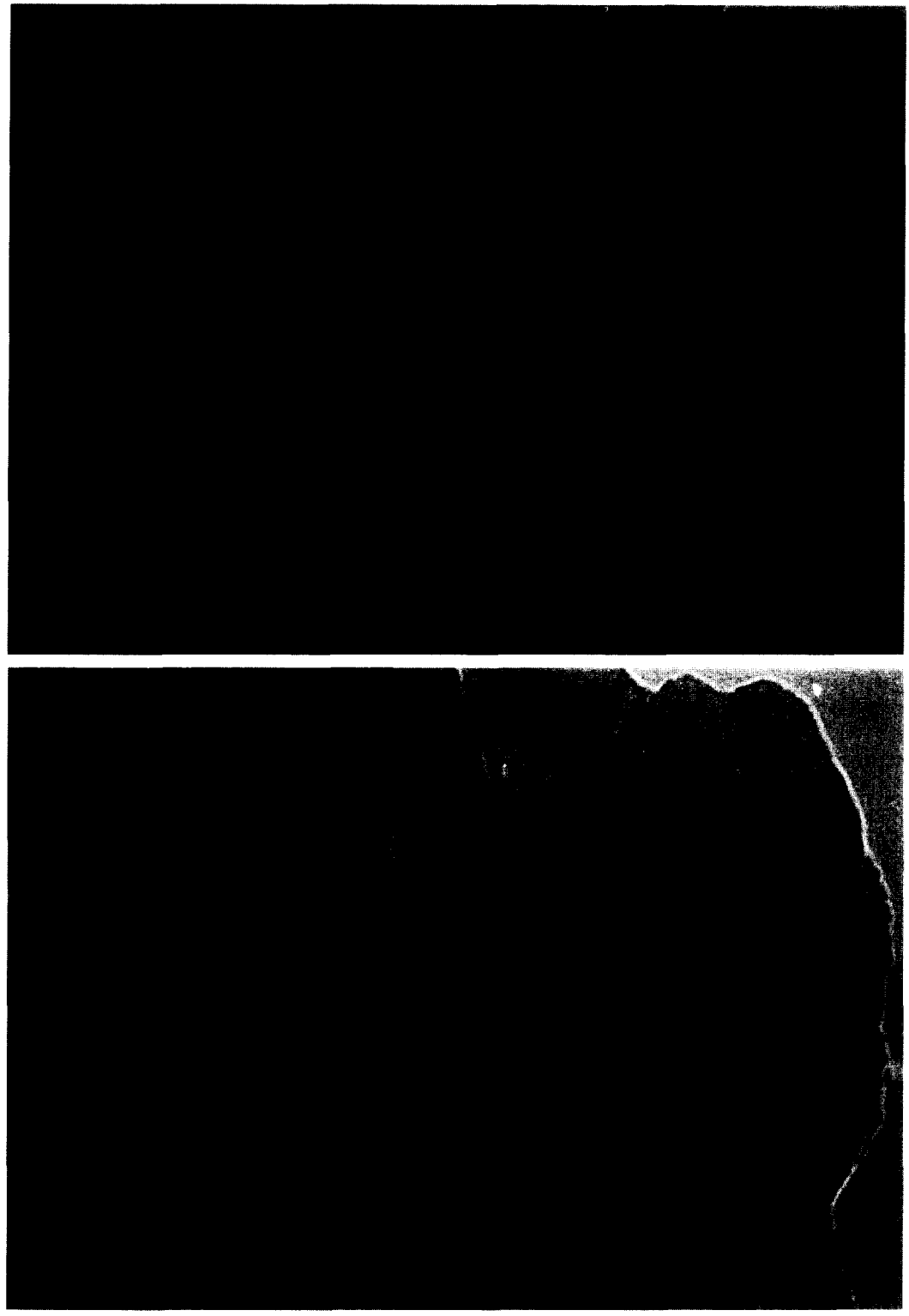

Fig. 9. High resolution electron micrographs typical of calcination products (anatase) obtained: (A) at low acid ratio, P(1:1:0.125); (B) at high acid ratio, P(1:1:1). Voids can be seen within the fused particle structure.

of acetic acid to titanium alkoxide has previously been reported to result in the formation of a co-polymerized gel [24]. Gel formation was explained in terms of the functionality of the formed $Ti(alkoxy)_3(OAc)$, which is smaller than that of $Ti(alkoxy)_4$; the more (OAc) groups there are around the titanium, then the smaller the functionality will be and, therefore, the slower the gelation will occur [25]. Applying these criteria to the present work then, slow polymerization would be expected to have occurred in the presence of acetic acid and could account for the extensive networks of fused crystallites comprising the products. We could argue further that, due to the decreased functionality of these materials, they tend to polymerize according to model (a) in Section 4.2.1.

Thus the decrease in the S_{BET} of the materials prepared in the presence of the low acid ratio, H(1:1:0.125), may be explained in terms of the decrease of porosity (see Table 2) due to the evolution from a low cross-linked gel. A further increase in the acetic acid ratio will lead to a further decrease in the cross-linking and, consequently, to a further drop in the S_{BET}, down to 20 $m^2 g^{-1}$ for H(1:1:0.25). The observed spherical particles of low porosity (Fig. 7(A)) may explain the drop in surface area. However, the re-increase of the surface area for the material prepared with high acid ratio, H(1:1:1), may be due to the inclusion of more acetate ligands in the gel skeleton. This, together with the low functionality in this case, may result in increasing porosity when the gel skeleton approaches the xerogel structure.

The similar trends of S_{BET} values observed for the "P"-type materials prepared in the presence of the acid may likewise be explained as above. Nevertheless, the low condensation rate in isopropanol should be kept in mind, as it would lead to a better polymerization (see Fig. 9(A) and Fig. 9(B)), and low surface area (see Table 2).

5. Conclusion

The effects of the preparation variables on the hydrolysis products of $Ti(OPr^i)_4$ and on the surface texture of the resultant titanias are as follows.

5.1. The solvent

n-Heptane is an aprotic solvent in which fast aggregation occurs, and open bulk structures result. Consequently, titanias of high surface area and inter-particle porosity are obtained. Isopropanol is a protic solvent, in which slow aggregation occurs, and compact bulk structures result giving rise to titanias of low surface area and intra-particle porosity.

5.2. Water ratio

Water in *n*-heptane causes heterogeneous hydrolysis, slight surface area increase with other properties remaining essentially unchanged. Water in isopropanol leads to homogeneous hydrolysis, increase in depolymerization, decrease in aggregation rate, and increase in bulk compactness and particle size.

5.3. Acid additives

These modify the nature of the alkoxide to give a hydrolysable product of lower functionality. Acetic acid addition to *n*-heptane tends to encourage spheroidal particles at low acid ratios; at high acid ratios gelation increases, resulting in irregularly shaped particles. In isopropanol the acid increases the solubility of the hydrolysed species, and decreases the polymerization rate: this gives rise to better gelation resulting in intra-particle porosity.

Acknowledgment

One of us (K.M.S.K.) thanks the Egyptian Ministry of Education for a grant that made possible an extended stay at Glasgow University.

References

[1] A.K. Datye, G. Riegel, J.R. Bolton, M. Huang, M.R. Prairie, J. Solid State Chem. 115 (1995) 236.
[2] S. Karmakar, H.L. Greene, J. Catal. 151 (1995) 394.

[3] M.J. Holgado, A.C. Inigo, V. Rives, React. Kinet. Catal. Lett. 54 (1995) 297.
[4] K.N.P. Kumar, Appl. Catal. A: 119 (1994) 163.
[5] G. Dagan, S. Sampath, O. Lev, Chem. Mater. 7 (1995) 446.
[6] M. Visca, E. Matijevic, J. Colloid Interface Sci. 68 (1979) 304.
[7] F. Kirkbir, H. Komiyama, J. Chem. Soc. Jpn., (1988) 791.
[8] K. Morishige, F. Kanno, S. Ogawara, S. Sasaki, J. Phys. Chem. 89 (1985) 4404.
[9] E.A. Barringer, H.K. Bowen, Langmuir 1 (1985) 414.
[10] I. Georgiadou, N. Spanos, C. Papadopoulou, H. Matralis, C. Kordulis, A. Lycourghiotis, Colloids Surf. A: 98 (1995) 155.
[11] D. Segal, Chemical Synthesis of Advanced Ceramic Materials, Cambridge University Press, Cambridge, 1989.
[12] H. Schmidt, J. Non-Cryst. Solids 100 (1988) 51.
[13] R.C. Mehrotra, J. Non-Cryst. Solids 100 (1988) 1.
[14] C. Sanchez, J. Livage, M. Henry, F. Babonneau, J. Non-Cryst. Solids 100 (1988) 65.
[15] J.V. Smith (Ed.), X-ray Powder Data File, American Society for Testing and Materials, Philadelphia, USA, 1960.
[16] B. Brunauer, P.H. Emmett, E. Teller, J. Am. Chem. Soc. 60 (1938) 309.
[17] International Union of Pure and Applied Chemistry, IUPAC, Pure Appl. Chem., 57 (1985) 603.
[18] A. Lecloux, J.P. Pirard, J. Colloid Interface Sci. 70 (1979) 265.
[19] S.J. Gregg, in: J. Rouquerol, K.S.W. King (Eds.), Adsorption at the Gas–Solid and Liquid–Solid Interfaces, Elsevier, Amsterdam, 1982, pp. 153–164.
[20] I. Laaziz, A. Larbot, A. Julbe, C. Guizard, L. Cot, J. Solid State Chem. 98 (1992) 393.
[21] D.C. Bradley, R.C. Mehrotra, D.P. Gaur, Metal Alkoxides, Academic Press, New York, 1978, p. 202.
[22] C.G. Brinker, G.W. Scherer, J. Non-Cryst. Solids 70 (1985) 301.
[23] K.C. Chen, T. Tsuchiya, J.D. Mackenzie, J. Non-Cryst. Solids 81 (1986) 227.
[24] S. Doeuff, M. Henry, C. Sanchez, J. Livage, J. Non-Cryst. Solids 89 (1987) 206.
[25] D.L. Trimm, Design of Industrial Catalysts, Oxford University Press, New York, 1984.